EXTENDED BOUSSINESQ EQUATIONS FOR WAVES IN POROUS MEDIA: DERIVATION OF GOVERNING EQUATIONS AND GENERATION OF WAVES INTERNALLY

Changhoon Lee[1] Van Nghi Vu[2] and Tae-Hwa Jung [3]

In this study we develop a new extended Boussinesq model that predicts the propagation of water waves in porous media. The inertial and drag resistances are taken account into the model in which the results are the same with the extended Boussinesq equations of Madsen and Sorensen (1992) when these resistances are removed. The developed model introduces its simplicity in solving the matching conditions at the permeable breakwater interfaces. The whole computational domain can be involved by specifying the porosity equal to unity outside the breakwater and to a value below unity inside the breakwater. There is no need for using any matching conditions at the interface. Furthermore, the applications of this current developed model are also extended to the cases that waves propagate inside and/or over a porous layer. For verification of the developed model, the internal generation of wave technique is applied to simulate sinusoidal and cnoidal waves propagating inside porous media in shallow and deep waters and nonlinear cnoidal waves interacting with porous breakwater. Numerical results give a good agreement with analytical solutions. Transformation of solitary waves to porous breakwater is also carried out. Refraction and transmission of solitary waves to the porous breakwater are well captured and verified by available physical experimental data.

Keywords: internal generation of wave, source function, energy dissipation, porous media, extended Boussinesq equations

INTRODUCTION

Wave energy dissipation through the rubble-mound breakwater happens by friction of water through permeable media and also by turbulence of high speed waters. It is hard to accurately predict the energy dissipation because the flow is micro-scale three-dimensional phenomenon. This was analytically investigated by Sollitt and Cross (1972). They assumed the flow resistance in the porous material is of the type of Forchheimer (1901). They solved for a damping wave component within the breakwater and matched boundary conditions at the sea-side and land-side faces of the breakwater to predict the reflected and transmitted wave components. An approximate solution to a rubble-mound breakwater was formulated in terms of an equivalent rectangular breakwater. Recently, Liu and Li (2013) derived a new analytical solution for wave reflection and transmission by a surface-piercing porous breakwater based on the classical porous medium model of Sollitt and Cross (1972). The advantage of this solution is its simplicity so that they do not need to use complex wave numbers for wave motion through porous media.

The wave dynamics through the rubble-mound breakwater has the following characteristics. There exist the regions 1 and 3 which respectively include sea- and land-side faces, of the breakwater. In these regions, waves are shoaling on the breakwater face and wave energy is dissipating under the breakwater face. In region 2 the water surface is inside the breakwater between the regions 1 and 3. In the region 2, wave energy is dissipating through the permeable materials and this region contains multiple layers of different permeability, i.e., a layer of crushed stones and a layer of armor units, as highlighted in Fig. 1. Energy dissipation through the breakwater would be different depending on the direction of incoming waves.

There are 2 types of governing equations to simulate waves propagating inside or over permeable layer. The first type of is the Boussinesq equations (Cruz et al., 1997; Liu and Wen, 1997; Hsiao et al., 2002, 2010) while the second type is the Navier-Stoke equations (Liu et al., 1999; del Jesus et al., 2012; Ma et al., 2014). Both types of governing equations consider energy dissipation by friction and turbulence. However, the latter is very time-consuming to simulate horizontally two-dimensional phenomenon such as refraction and diffraction.
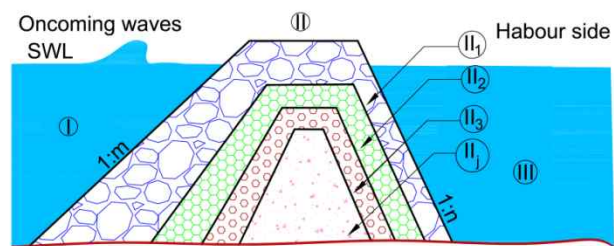

Figure 1. Computational domain

Liu and Wen (1997) and Lynett et al. (2000) developed Boussinesq equations for waves propagating inside porous media which considers laminar and turbulent resistances. However, they did

[1]Dept. of Civil & Environmental Engineering, Sejong University, Seoul 143-747 Korea.
[2]Dept. of Civil & Environmental Engineering, Sejong University, Seoul 143-747 Korea.
[3] Dept. of Civil Engineering, Hanbat National University, Daejeon 305-719, Korea.

not consider the inertial effect. When the drag resistance is neglected, this model is reduced to the equations of Peregrine (1967) which can be applied only in shallow water.

In section 2 we develop the Boussinesq equations for waves inside a permeable layer. As our review on previous studies, the wave models for permeable layers (Madsen et al., 1997; Kennedy et al., 2000) do not take into account the characteristics of waves inside the permeable layers such as the laminar and turbulent resistances, and the effects caused by the porosity and added mass coefficient. All those characteristics are considered in both Cruz et al.'s and the presently derived Boussinesq equations. The developed model is reduced to the equations of Madsen and Sorensen (1992) which can be applied in deeper water given that these resistances are neglected. In section 3, the authors derive the source function using Green's function approach to generate waves internally in a permeable layer. Section 4 shows some numerical experiments in horizontal 1-dimensional domain to verify our developed theory. Numerical results are compared to analytical solutions and physical experiments. Sinusoidal, solitary, and cnoidal waves are simulated to propagate inside porous media and through a porous breakwater. Section 5 summarize and conclude the present works.

DEVELOPMENT OF EXTENDED BOUSSINESQ EQUATIONS IN POROUS MEDIA

We apply boundary conditions to develop the Boussinesq equations for waves propagating inside porous media in shallow water area and then the developed equations are extended to deeper water for more application.

Setting-up boundary value problem

The whole domain is vertically divided into the 1st, 2nd,..., and $J-th$ layers which are numbered from the top to the bottom layers with different porosities, as shown in Fig. 2. The free surface is located at the 1st layer.

Since the porosity is uniform, the continuity equation inside the $j-th$ permeable layer is given by

Figure 2. Porous media

$$\nabla_3 \cdot \mathbf{U}_j = 0 \qquad (1)$$

where $\mathbf{U} = (u, v, w)$ is the seepage velocity vector, $\nabla_3 \equiv (\partial/\partial x, \partial/\partial y, \partial/\partial z)$ is the gradient operator, and the subscript j implies the $j-th$ layer. The momentum equation inside the $j-th$ permeable layer is given by

$$\frac{d\mathbf{U}_j}{dt} + \frac{1}{\rho}\nabla_3\left(p_j + \rho g z\right) + D_j + I_j = 0 \qquad (2)$$

where p_j is the pore pressure, D_j and I_j are the drag and inertial resistance terms, respectively. It should be noted that the continuity equation (1) and momentum equation (2) are expressed in terms of the seepage velocity of the pore water. Several people defined the drag resistance term differently. Ergun (1952) define the drag resistance term in the Forchheimer (1901) type using a volume-averaged discharge velocity $\mathbf{U}_j'\left(= \lambda_j \mathbf{U}_j\right)$. In our study, we use Ergun's definition of D in terms of the seepage velocity instead as

$$
\begin{aligned}
D_j &\equiv \left[\alpha_l\left(\frac{1-\lambda}{\lambda}\right)^2\frac{\nu}{d^2}\frac{\mathbf{U}'}{\lambda} + \alpha_t\frac{1-\lambda}{\lambda}\frac{1}{d}\left|\frac{\mathbf{U}'}{\lambda}\right|\frac{\mathbf{U}'}{\lambda}\right]_j \\
&= \left[\alpha_l\left(\frac{1-\lambda}{\lambda}\right)^2\frac{\nu}{d^2}\mathbf{U} + \alpha_t\frac{1-\lambda}{\lambda}\frac{1}{d}\left|\mathbf{U}\right|\mathbf{U}\right]_j
\end{aligned}
\qquad (3)
$$

where α_l and α_t are coefficients which represent the laminar and turbulent flow resistances, respectively, ν is the kinematic viscosity of water, and d is the size of the solid. The inertial resistance term I_j is given by
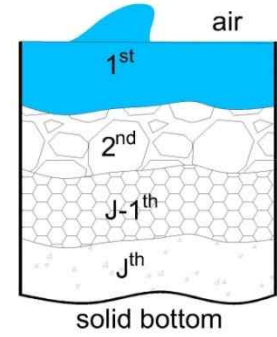
$$I_j \equiv \left[(1-\lambda)(1+\kappa) \frac{d\mathbf{U}}{dt} \right]_j \tag{4}$$

where λ is the porosity, and κ is the added mass coefficient.

Several people proposed different momentum equations in including the drag and inertial resistance terms. Sollitt and Cross' (1972) momentum equation is the same as the present momentum equation (2) except that the convective acceleration is neglected to get a linear solution. Substitution of Eqs. (3) and (4) into the present momentum equation (2) gives

$$\beta_j \frac{d\mathbf{U}_j}{dt} + \frac{1}{\rho} \nabla_3 \left(p_j + \rho g z \right) + \alpha_j \mathbf{U}_j = 0 \tag{5}$$

where β_j is the inertial coefficient given by

$$\beta_j \equiv \left[1 + (1-\lambda)(1+\kappa) \right]_j \tag{6}$$

and α_j is the drag coefficient given by

$$\alpha_j = \left[\alpha_l \left(\frac{1-\lambda}{\lambda} \right)^2 \frac{\nu}{d^2} + \alpha_t \frac{1-\lambda}{\lambda} \frac{1}{d} |\mathbf{U}| \right]_j \tag{7}$$

At the free surface, the dynamic and kinematic boundary conditions are given by

$$p_1 = 0, \qquad z = \eta \tag{8}$$

$$w_1 = \frac{\partial \eta}{\partial t} + \mathbf{u}_1 \cdot \nabla \eta, \qquad z = \eta \tag{9}$$

where $\mathbf{u} \equiv (u,v)$ is the horizontal velocity vector and $\nabla \equiv (\partial/\partial x, \partial/\partial y)$ is the horizontal gradient operator. At the impermeable bottom under the lowest $J-th$ layer, the normal velocity vanishes as

$$\mathbf{U}_J \cdot \nabla_3 \left(z + h_J \right) = w_J + \mathbf{u}_J \cdot \nabla h_J = 0, \qquad z = -h_J \tag{10}$$

At the interface between the $j-th$ and $(j+1)-th$ layers, both the pore pressures at and normal fluxes through the interface are continuous as

$$p_j = p_{j+1}, \qquad z = -h_j \tag{11}$$

$$\lambda_j \left(w_j + \mathbf{u}_j \cdot \nabla h_j \right) = \lambda_{j+1} \left(w_{j+1} + \mathbf{u}_{j+1} \cdot \nabla h_j \right), \qquad z = -h_j \tag{12}$$

We get the Boussinesq equations by specifying the boundary value problem with a governing equation and boundary conditions. The seepage velocity potential is defined as

$$\mathbf{U}_j \equiv \nabla_3 \Phi_j \tag{13}$$

The variables are normalized using the relevant characteristic length and time as

$$x' = \frac{x}{l}, \quad y' = \frac{y}{l}, \quad z' = \frac{z}{h_0}, \quad h' = \frac{h}{h_0}, \quad \eta' = \frac{\eta}{a}, \quad t' = \frac{\sqrt{gh_0}}{l}t,$$

$$\Phi' = \frac{h_0}{al\sqrt{gh_0}}\Phi, \quad u' = \frac{h_0}{a\sqrt{gh_0}}u, \quad \alpha' = \frac{l}{\sqrt{gh_0}}\alpha$$

$$(14)$$

where l is the wavelength, h_0 is the maximum water depth, a is the maximum amplitude of the water surface elevation, t is the wave period. When the normalization is applied, the terms in the governing equation and boundary conditions will group according to two non-dimensional quantities

$$\varepsilon = \frac{a}{h_0}, \qquad \mu = \frac{h_0}{l}$$

$$(15)$$

where ε is the nonlinearity parameter and μ is the dispersivity parameter. Omitting the primes for convenience, the continuity equation (1) and boundary conditions (8)-(12) become, respectively,

$$\mu^2\nabla^2\Phi_j + \frac{\partial^2\Phi_j}{\partial z^2} = 0, \qquad -1 < z < \varepsilon\eta$$

$$(16)$$

$$\mu^2\left(\beta_1\frac{\partial\Phi_1}{\partial t} + \alpha_1\Phi_1 + \eta\right) + \varepsilon\beta_1\frac{1}{2}\left[\mu^2\left(\nabla\Phi_1\right)^2 + \left(\frac{\partial\Phi_1}{\partial z}\right)^2\right] = 0, z = \varepsilon\eta$$

$$(17)$$

$$\frac{\partial\Phi_1}{\partial z} = \mu^2\left(\frac{\partial\eta}{\partial t} + \varepsilon\nabla\Phi_1\cdot\nabla\eta\right), \qquad z = \varepsilon\eta$$

$$(18)$$

$$\frac{\partial\Phi_J}{\partial z} = -\mu^2\nabla\Phi_J\cdot\nabla h_J, \qquad z = -h_J$$

$$(19)$$

$$\mu^2\left(\beta_j\frac{\partial}{\partial t} + \alpha_j\right)\Phi_j + \varepsilon\beta_j\frac{1}{2}\left[\left(\frac{\partial\Phi_j}{\partial z}\right)^2 + \mu^2\left(\nabla\Phi_j\right)^2\right]$$

$$= \mu^2\left(\beta_{j+1}\frac{\partial}{\partial t} + \alpha_{j+1}\right)\Phi_{j+1} + \varepsilon\beta_{j+1}\frac{1}{2}\left[\left(\frac{\partial\Phi_{j+1}}{\partial z}\right)^2 + \mu^2\left(\nabla\Phi_{j+1}\right)^2\right], z = -h_j$$

$$(20)$$

$$\lambda_j\left(\frac{\partial\Phi_j}{\partial z} + \mu^2\nabla\Phi_j\cdot\nabla h_j\right)$$

$$= \lambda_{j+1}\left(\frac{\partial\Phi_{j+1}}{\partial z} + \mu^2\nabla\Phi_{j+1}\cdot\nabla h_{j+1}\right), \qquad z = -h_j$$

$$(21)$$

The velocity potential is assumed to be expressed as a power series in the vertical coordinate given by

$$\Phi_j\left(x,y,z,t\right) = \sum_{n=0}^{\infty}\left[z + h_j\left(x,y\right)\right]^n\varphi_{j,n}\left(x,y,t\right)$$

$$(22)$$

Then, the continuity equation (16) becomes

$$(n+1)(n+2)\left[1 + \mu^2\left(\nabla h_j\right)^2\right]\varphi_{j,n+2}$$

$$+(n+1)\mu^2\left[2\nabla h_j\cdot\nabla\varphi_{j,n+1} + \nabla^2 h_j\,\varphi_{j,n+1}\right] + \mu^2\nabla^2\varphi_{j,n} = 0, n = 0,1,2,\cdots$$

$$(23)$$

and the bottom boundary condition (19) becomes

$$\varphi_{J,1} = -\mu^2 \frac{\nabla h_J \cdot \nabla \varphi_{J,0}}{1 + \mu^2 \left(\nabla h_J\right)^2}$$

(24)

And, the velocity potential functions in the lowest layer $\varphi_{J,2}$, $\varphi_{J,3}$, $\cdots$ can be expressed in terms of $\varphi_{J,0}$ and thus the velocity potential in the bottom layer Φ_J can be expressed to the order of $O\left(\mu^2\right)$ as

$$\Phi_J = \varphi_{J,0} - \frac{\mu^2}{2}\left[2(z + h_J)\nabla h_J \cdot \nabla \varphi_{J,0} + (z + h_J)^2 \nabla^2 \varphi_{J,0}\right] + O\left(\mu^4\right)$$

(25)

Development of Boussinesq equations for waves inside one permeable layer

For one permeable layer, all the subscripts j in the variables are $j = 1$. Thus, the velocity potential given by Eq. (25) becomes

$$\Phi_1 = \varphi_{1,0} - \frac{\mu^2}{2}\left[2(z + h_1)\nabla h_1 \cdot \nabla \varphi_{1,0} + (z + h_1)^2 \nabla^2 \varphi_{1,0}\right] + O\left(\mu^4\right)$$

(26)

The momentum equation is obtained by substituting Eq. (26) into the dynamic free-surface boundary condition (17) and then applying ∇ to the resulting equation as

$$\left(\beta_1 \frac{\partial}{\partial t} + \alpha_1\right)\left[u_{1,0} - \frac{\mu^2}{2}\nabla \cdot \left(h_1^2 \mathbf{u}_{1,0}\right)\right] + \nabla \eta + \varepsilon \beta_1 \mathbf{u}_{1,0} \cdot \nabla \mathbf{u}_{1,0} = 0$$

(27)

where $\mathbf{u}_{1,0} \equiv \nabla \varphi_{1,0}$ is the velocity at the bottom. Here, we use the depth-averaged velocity defined as

$$\overline{\mathbf{u}}_1 \equiv \frac{1}{h_1 + \varepsilon \eta}\int_{-h_1}^{\varepsilon \eta} \nabla \Phi_1 \, dz$$

(28)

And the drag coefficient α_j is defined again in terms of the depth-averaged horizontal velocity as

$$\alpha_j = \left(\alpha_l \left(\frac{1 - \lambda}{\lambda}\right)^2 \frac{\nu}{d^2} + \alpha_t \frac{1 - \lambda}{\lambda}\frac{1}{d}|\overline{\mathbf{u}}|\right)_j$$

(29)

After substituting Eq. (26) into Eq. (28), the velocity at the bottom can be expressed in terms of the depth-averaged velocity as

$$\overline{\mathbf{u}}_{1,0} = \overline{\mathbf{u}}_1$$
$$+ \frac{\mu^2}{2}\left[\begin{array}{l}\frac{h_1^2}{3}\nabla\left(\nabla \cdot \overline{\mathbf{u}}_1\right) + h_1 \nabla\left(\nabla h_1 \cdot \overline{\mathbf{u}}_1\right) \\ + h_1 \nabla h_1 \, \nabla \cdot \overline{\mathbf{u}}_1 + 2\nabla h_1 \, \nabla h_1 \cdot \overline{\mathbf{u}}_1\end{array}\right] + O\left(\mu^4\right)$$

(30)

Substitution of Eq. (30) into the momentum equation (27) gives

$$\left(\beta_1 \frac{\partial}{\partial t} + \alpha_1\right)\overline{\mathbf{u}}_1 + \nabla \eta + \varepsilon \beta_1 \overline{\mathbf{u}}_1 \cdot \nabla \overline{\mathbf{u}}_1$$
$$+ \frac{\mu^2}{2}\left(\beta_1 \frac{\partial}{\partial t} + \alpha_1\right)\left\{\frac{h_1^2}{3}\nabla\left(\nabla \cdot \overline{\mathbf{u}}_1\right) - h_1 \nabla\left[\nabla \cdot \left(h_1 \, \overline{\mathbf{u}}_1\right)\right]\right\} = 0$$

(31)

The continuity equation is obtained by substituting Eq. (26) into the kinematic free-surface boundary condition (18) as

$$\frac{\partial \eta}{\partial t} + \nabla \cdot \left[\left(h_1 + \varepsilon \eta\right)\overline{\mathbf{u}}_1\right] = 0$$

(32)

Eqs. (47) and (48) are the set of Boussinesq equations for waves inside one permeable layer in non-dimensional form. In physical variables, the equations are

$$\left(\beta_1 \frac{\partial}{\partial t} + \alpha_1\right)\overline{\mathbf{u}}_1 + g\nabla\eta + \beta_1\,\overline{\mathbf{u}}_1 \cdot \nabla\overline{\mathbf{u}}_1$$

$$+\frac{1}{2}\left(\beta_1 \frac{\partial}{\partial t} + \alpha_1\right)\left\{\frac{h_1^2}{3}\nabla\left(\nabla\cdot\overline{\mathbf{u}}_1\right) - h_1\nabla\left[\nabla\cdot\left(h_1\,\overline{\mathbf{u}}_1\right)\right]\right\} = 0 \tag{33}$$

$$\frac{\partial\eta}{\partial t} + \nabla\cdot\left[\left(h_1 + \eta\right)\overline{\mathbf{u}}_1\right] = 0 \tag{34}$$

If the domain is not in porous media but in clean water ($\lambda_1 = 1$), then $\beta_1 = 1$ and $\alpha_1 = 0$, and thus the momentum equation (33) becomes

$$\frac{\partial\overline{\mathbf{u}}_1}{\partial t} + g\nabla\eta + \overline{\mathbf{u}}_1 \cdot \nabla\overline{\mathbf{u}}_1 + \frac{1}{2}\left\{\frac{h_1^2}{3}\nabla\left(\nabla\cdot\frac{\partial\overline{\mathbf{u}}_1}{\partial t}\right) - h_1\nabla\left[\nabla\cdot\left(h_1\frac{\partial\overline{\mathbf{u}}_1}{\partial t}\right)\right]\right\} = 0 \tag{35}$$

Eqs. (34) and (35) are the Boussinesq equations of Peregrine (1967) for waves on impermeable beds.

Development of extended Boussinesq equations for deeper waters

The developed Boussinesq equations can be applied in relatively shallow water, but cannot be applied in deeper waters. Since 1990s, several researchers have extended the Boussinesq equations which are applied to deeper waters for waves on impermeable beds (Madsen and Sorensen, 1992; Nwogu, 1993, Wei et al. 1995). For waves on permeable beds, Cruz et al. (1997) and Hsiao et al. (2002) followed the approaches of Madsen and Sorensen (1992), and Nwogu (1993), respectively, to extend their model for deeper waters. Here, Cruz et al.'s (1997) approach is employed to extend the model for deeper waters. Thus, the momentum equation (35) becomes

$$\left(\beta\frac{\partial}{\partial t} + \alpha\right)\overline{\mathbf{u}} + g\nabla\eta + \beta\,\overline{\mathbf{u}}\cdot\nabla\overline{\mathbf{u}} + \frac{1}{6}\left(\beta\frac{\partial}{\partial t} + \alpha\right)h^2\nabla\left(\nabla\cdot\overline{\mathbf{u}}\right)$$

$$-\left(\frac{1}{2} + \gamma\right)\left(\beta\frac{\partial}{\partial t} + \alpha\right)h\nabla\left[\nabla\cdot\left(h\overline{\mathbf{u}}\right)\right] - \gamma\,gh\nabla\left[\nabla\cdot\left(h\nabla\eta\right)\right] = 0 \tag{36}$$

where $\gamma = 1/15$ is a correction factor to improve the dispersion relation. Eqs. (34) and (36) are the extended Boussinesq equations for waves inside a permeable layer.

INTERNAL GENERATION OF WAVES IN POROUS MEDIA

Geometric optic approach

Neglecting nonlinear terms and considering waves propagating in one-dimensional domain over constant water depth, the extended Boussinesq equations for waves in a porous layer are simplified from Eqs. (34) and (36) as

$$\frac{\partial\eta}{\partial t} + h\frac{\partial u}{\partial x} = 0 \tag{37}$$

$$\left(\beta\frac{\partial}{\partial t} + \alpha\right)u + g\frac{\partial\eta}{\partial x} - \left(\gamma + \frac{1}{3}\right)\left(\beta\frac{\partial}{\partial t} + \alpha\right)h^2\frac{\partial^2 u}{\partial x^2} - \gamma\,gh^2\frac{\partial^3\eta}{\partial x^3} = 0 \tag{38}$$

Differentiating Eq. (38) in space and using Eq. (37) yields

$$\frac{\partial^2\eta}{\partial t^2} + \frac{\alpha}{\beta}\frac{\partial\eta}{\partial t} - \frac{gh}{\beta}\frac{\partial^2\eta}{\partial x^2} - \left(\gamma + \frac{1}{3}\right)h^2\frac{\partial^4\eta}{\partial x^2\partial t^2}$$

$$-\left(\gamma + \frac{1}{3}\right)\frac{\alpha}{\beta}h^2\frac{\partial^3\eta}{\partial x^2\partial t} + \frac{\gamma}{\beta}gh^3\frac{\partial^4\eta}{\partial x^4} = 0 \tag{39}$$

The water surface elevation can be expressed as

$$\eta = a_0 e^{i(kx-\omega t)} = a e^{i(k_r x-\omega t)} \tag{40}$$

where $a = a_0 e^{-k_i x}$, $k\left(= k_r + i k_i\right)$ is the complex wave number, k_r is the real part related to wave phase, and k_i is the imaginary part related to the decay of wave amplitude. Substituting Eq. (40) into Eq. (39) give, in real part, the phase velocity given by

$$C_p^2 = \left(\frac{\omega}{k_r}\right)^2$$

$$= gh \frac{1-\left(\frac{k_i}{k_r}\right)^2 - 6\gamma\left(k_r h\right)^2\left(\frac{k_i}{k_r}\right)^2 + \gamma\left(k_r h\right)^2\left[1+\left(\frac{k_i}{k_r}\right)^4\right]}{\beta\left\{1+\left(\gamma+\frac{1}{3}\right)\left(k_r h\right)^2\left[1-\left(\frac{k_i}{k_r}\right)^2\right]-2\left(\gamma+\frac{1}{3}\right)\frac{\alpha}{\beta\omega}\left(k_r h\right)^2\frac{k_i}{k_r}\right\}} \tag{41}$$

The imaginary part gives information of the energy velocity given by

$$C_e = \frac{\omega}{k_r} \frac{\beta\left\{1+\left(\gamma+\frac{1}{3}\right)\left(k_r h\right)^2\left[1-\left(\frac{k_i}{k_r}\right)^2\right]\right\}-2\left(\gamma+\frac{1}{3}\right)\frac{\alpha}{\omega}\left(k_r h\right)^2\frac{k_i}{k_r}}{\beta\left\{1+\left(\gamma+\frac{1}{3}\right)\left(k_r h\right)^2\left[1-\left(\frac{k_i}{k_r}\right)^2\right]\right\}-\left(\gamma+\frac{1}{3}\right)\frac{\alpha}{\omega}\left(k_r h\right)^2\frac{k_i}{k_r}}$$

$$\times \frac{1-\left(\gamma+\frac{1}{3}\right)\frac{\omega^2 h}{g}\left(\beta-\frac{\alpha}{\omega}\frac{k_i}{k_r}\right)+2\gamma\left(k_r h\right)^2\left[1-3\left(\frac{k_i}{k_r}\right)^2\right]}{1-\left(\frac{k_i}{k_r}\right)^2 - 6\gamma\left(k_r h\right)^2\left(\frac{k_i}{k_r}\right)^2 + \gamma\left(k_r h\right)^2\left[1+\left(\frac{k_i}{k_r}\right)^4\right]} \tag{42}$$

For waves propagating in clean water media (i.e., $\beta = 1$, $\alpha = 0$), Eq. (42) reduces to the energy velocity of the extended Boussinesq equations of Madsen and Sorensen (1992) derived by Kim et al. (2007).

The relation between non-dimensional wavenumber and characteristic of porous media is specified as

$$\frac{\alpha}{\omega}\left\{1+\left(\gamma+\frac{1}{3}\right)\left(k_r h\right)^2\left[1-\left(\frac{k_i}{k_r}\right)^2\right]\right\}$$

$$= 2\frac{k_i}{k_r}\left\{1-\left(\gamma+\frac{1}{3}\right)\beta\frac{\omega^2 h}{g}+4\gamma\left(k_r h\right)^2\left[1-\left(\frac{k_i}{k_r}\right)^2\right]\right\}$$

$$\times \frac{\beta\left\{1+\left(\gamma+\frac{1}{3}\right)\left(k_r h\right)^2\left[1-\left(\frac{k_i}{k_r}\right)^2\right]\right\}-2\left(\gamma+\frac{1}{3}\right)\frac{\alpha}{\omega}\left(k_r h\right)^2\frac{k_i}{k_r}}{1-\left(\frac{k_i}{k_r}\right)^2 - 6\gamma\left(k_r h\right)^2\left(\frac{k_i}{k_r}\right)^2 + \gamma\left(k_r h\right)^2\left[1+\left(\frac{k_i}{k_r}\right)^4\right]} \tag{43}$$

Derivation of source function

A mass source function S_M is added to the continuity equation (37). Differentiating the momentum equation (38) in space and using Eq. (37) with the mass source function S_M yields

$$-\left(\beta\frac{\partial}{\partial t}+\alpha\right)\frac{1}{h}\frac{\partial\eta}{\partial t}+g\frac{\partial^2\eta}{\partial x^2}+\left(\gamma+\frac{1}{3}\right)\left(\beta\frac{\partial}{\partial t}+\alpha\right)h\frac{\partial^3\eta}{\partial x^2\partial t}-\gamma\,gh^2\frac{\partial^4\eta}{\partial x^4}$$

$$=-\left(\beta\frac{\partial}{\partial t}+\alpha\right)\frac{S}{h}+\left(\gamma+\frac{1}{3}\right)\left(\beta\frac{\partial}{\partial t}+\alpha\right)h\frac{\partial^2 S_M}{\partial x^2}$$

(44)

The time-harmonic term can be separated as

$$\eta(x,t)=\tilde{\eta}(x)\exp(-i\omega t)$$

(45)

$$S_M(x,t)=\tilde{S}_M(x)\exp(-i\omega t)$$

(46)

Substituting the time-harmonic terms given by Eqs. (45) and (46) into Eq. (44) yields a fourth-order ordinary differential equation

$$C_1\frac{d^4\tilde{\eta}}{dx^4}+C_2\frac{d^2\tilde{\eta}}{dx^2}+C_3\tilde{\eta}=C_4\tilde{S}_M$$

(47)

where

$$C_1=-\gamma\,gh^3$$

(48)

$$C_2=gh\left[1-\left(\gamma+\frac{1}{3}\right)\left(\beta+i\frac{\alpha}{\omega}\right)\frac{\omega^2 h}{g}\right]$$

(49)

$$C_3=\left(\beta+i\frac{\alpha}{\omega}\right)\omega^2$$

(50)

$$C_4=i\omega\left(\beta+i\frac{\alpha}{\omega}\right)\left[1-\left(\gamma+\frac{1}{3}\right)h^2\frac{d^2}{dx^2}\right]$$

(51)

Following Wei et al. (1999) we apply Green's function approach to Eq. (47) to get the surface elevation as

$$\tilde{\eta}(x)=\frac{1}{2}\frac{\omega}{k_r}\frac{1}{gh}\frac{I_1}{f}\exp\left[k_r\left(1+i\frac{k_i}{k_r}\right)(x-x_s)\right]$$

(52)

where f is a function of dimensionless terms (i.e., $k_r h,\ k_i/k_r,\dots$), defined as

$$f=\frac{1+i\dfrac{k_i}{k_r}}{\beta+i\dfrac{\alpha}{\omega}}\frac{1-\left(\gamma+\dfrac{1}{3}\right)\dfrac{\omega^2 h}{g}\left(\beta+i\dfrac{\alpha}{\omega}\right)+2\gamma\left(k_r h\right)^2\left(1+i\dfrac{k_i}{k_r}\right)^2}{1+\left(\gamma+\dfrac{1}{3}\right)\left(k_r h\right)^2\left(1+i\dfrac{k_i}{k_r}\right)^2}$$

(53)

$$I_1=\sqrt{\frac{\pi}{\beta}}\exp\left[-\frac{\left(k_r+ik_i\right)^2}{4\beta}\right]$$

(54)

The target surface elevation is given by

$$\tilde{\eta}(x) = a_0 \exp\left[k_r \left(1 + i \frac{k_i}{k_r} \right)(x - x_s) \right] \tag{55}$$

By comparing Eq. (52) with the target surface elevation in Eq. (55) we can get the source function as

$$S_M = 2\eta^I g h \frac{k_r}{\omega} f \frac{\exp\left[-\beta_0 (x - x_s)^2 \right]}{I_1} \tag{56}$$

NUMERICAL VERIFICATION

This section verifies our developed model by simulating wave propagation in different porous media and comparing numerical results with the exact solution and physical experiments.

Numerical scheme

A finite-difference model is introduced to solve the extended Boussinesq equations for waves propagating in a porous layer. A 4th-order Adams-Basthforth-Moulton predictor and corrector scheme is employed to discretize the model equations in time. The first-order spatial derivative terms are differenced to $O(\Delta x^4)$ utilizing a five-point formula. Spatial and temporal differencing of the higher-order dispersion terms is done to the second-order accuracy. We apply numerical scheme the same as FUNWAVE 1.0 (Kirby et al., 1998) model with predictor and corrector steps. The predictor step is the third-order explicit Adams-Bashforth scheme and the corrector step applies the fourth-order implicit Adams-Moulton. The corrector step is iterated until the error between two successive results smaller than a required limit (i.e., 10^{-5}).

Sponge layers are placed at the outside boundaries of the computation domain in order to dissipate wave energy inside the sponge layers. Thus, the momentum equation (36) is modified as

$$\left(\beta \frac{\partial}{\partial t} + \alpha \right)\mathbf{u} + g\nabla\eta + \beta\mathbf{u}\cdot\nabla\mathbf{u} + \frac{1}{6}\left(\beta \frac{\partial}{\partial t} + \alpha \right)h^2\nabla(\nabla\cdot\mathbf{u})$$
$$-\left(\frac{1}{2} + \gamma \right)\left(\beta \frac{\partial}{\partial t} + \alpha \right)h\nabla\left[\nabla\cdot(h\mathbf{u}) \right] - \gamma g h\nabla\left[\nabla\cdot(h\nabla\eta) \right] + \omega D_s\mathbf{u} = 0 \tag{57}$$

where D_s is the damping coefficient inside the sponge layer given by

$$D_s = \begin{cases} 0, & \text{outside sponge layer} \\ \omega \dfrac{\exp\left[(d/Sp)^{2.5} \right] - 1}{\exp(1) - 1}, & \text{inside sponge layer} \end{cases} \tag{58}$$

where Sp is the sponge layer thickness as $Sp = 4L_0$ (L_0 is the wavelength without damping) and d is the distance from the starting point of the sponge layer. In order to generate wave smoothly, a hyperbolic tangent function $\tanh(n\Delta t/5T)$, where n is the time stage, Δt is the time step and T is wave period, is multiplied to the source function.

Sinusoidal waves propagation inside porous media

Waves are simulated to propagate in shallow ($kh = 0.09\pi$) and deep ($kh = 1.2\pi$) waters in horizontal 1-dimensional domain. The source function width is one wavelength, and the width of the sponge layer is 4 wavelengths. The grid size is chosen as $\Delta x = L_0/50$, and the time step is chosen to guarantee stable solution with Courant number $C_r = 0.1$.

We use the values of drag resistance from Ergun's (1952) as $\alpha_l = 150$, $\alpha_t = 1.75$, $\kappa = 0.4$. In this section we generate waves in different porous media by changing the porosity λ and the porous material diameter d. The water depth is kept constant $h = 2m$.

Fig. 3 compares numerical and analytical solutions of normalized wave amplitudes. The analytical solution is determined as $\exp(-k_i x)$. A good agreement is observed from this comparison. Besides

that, by comparing waves propagate in shallow porous media (Figs. 3**Figure** (a1), (a2), (a3)) with deep porous media (Figs. 3 (b1), (b2), (b3)), it can be seen that with the same porosity characteristics, the wave amplitude in shallow water is dissipated more than the wave amplitude in deep area. At the same water depth, if the porosity is constant the energy dissipation increases while the porous material diameter decreases (i.e., by comparing Figs. 3 (a1) and (a2), and Figs. 3 (b1) and (b2)), if the porous material diameter is constant the energy dissipation increases while the porosity decreases (i.e., by comparing Figs. 3 (a3) and (a2), and Figs. 3 (b3) and (b2)).
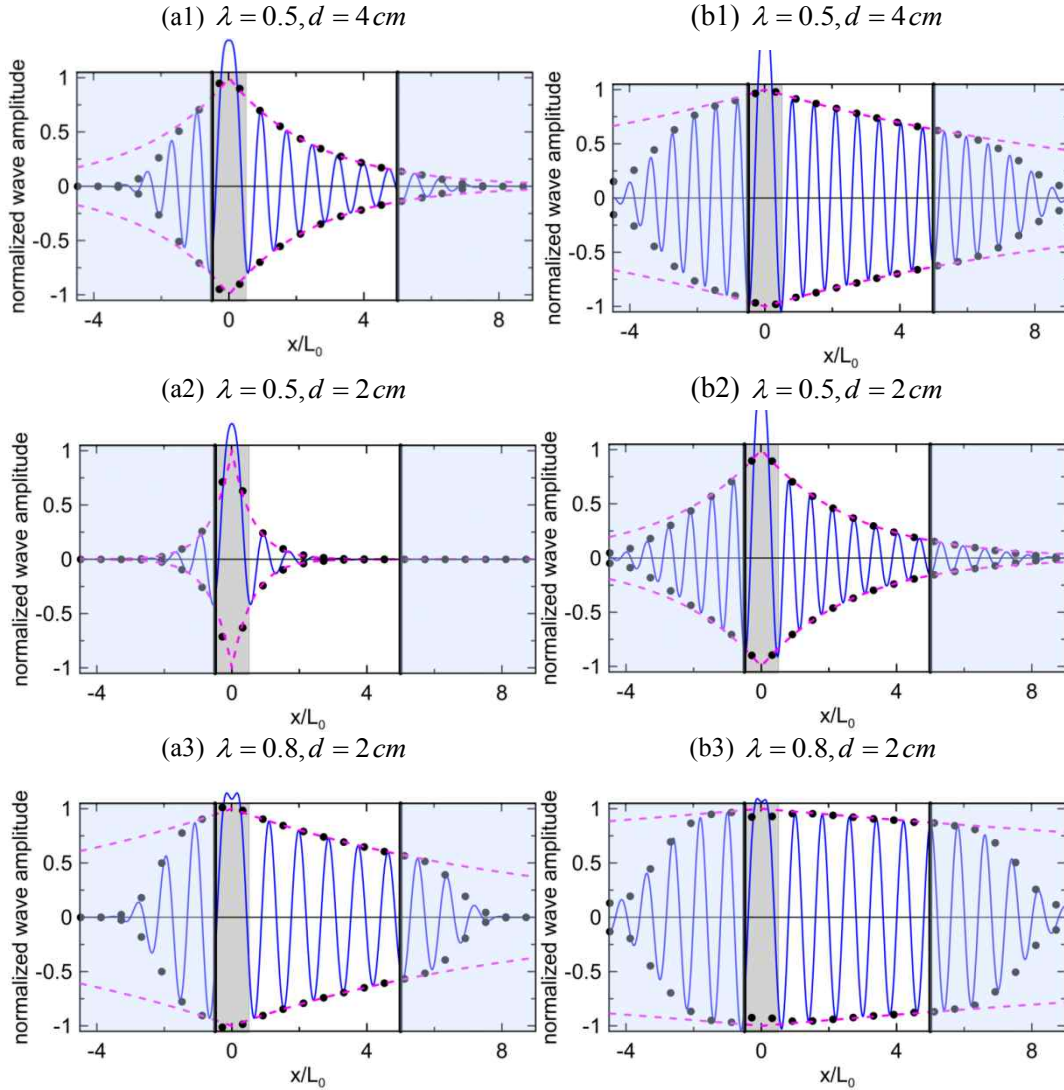

Figure 3. Comparison of normalized wave amplitudes. Line definition: filled-circle = numerical amplitude, solid line = surface elevation; dashed-line = exact solution, vertical bold line = starting point of sponge layer, shaded rectangle = source region. (a1) – (a3): $kh = 0.09\pi$, (b1) – (b3): $kh = 1.2\pi$.

Generation of Cnoidal waves in porous media

In the previous section source function method was developed for linear waves propagating inside porous media. In this section we generate nonlinear cnoidal waves for horizontally one-dimensional porous media. The surface elevation of incident cnoidal waves is given by

$$\eta^I = \eta_t + H cn^2 \left(2K \frac{t}{T} \Big| m \right)$$

(59)

where η_t is the elevation of wave trough,

$$\eta_t = \frac{H}{m}\left(1 - m - \frac{E}{K}\right) \tag{60}$$

where H is the incident wave height, cn is the Jacobian elliptic function, K is the complete elliptic integral of the first kind, E is the complete elliptic integral of the second kind, and m is the modulus which determines the wave shape.

In the numerical simulation, the water depth is chosen as $10\,m$, and the wave period is $20\,s$ which cause relative shallow water depth with $kh = 0.1\pi$. At each time step the surface elevation of cnoidal wave is added to the model. The added surface elevation of cnoidal wave is given by Cho (2003).
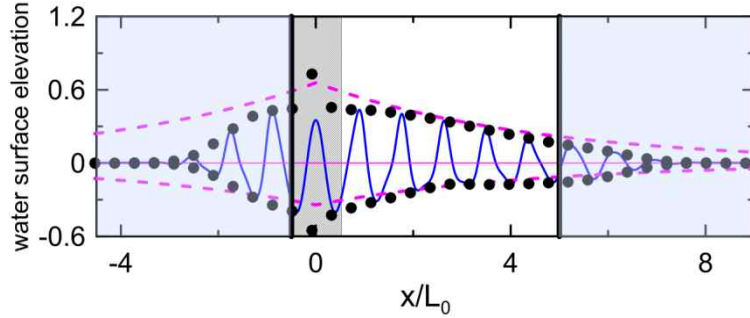

Figure 4. Comparison of numerical solution of Cnoidal waves with exact solution. Line def.: same as Fig. 3.

The characteristics of the porous media are $\alpha_l = 150$, $\kappa = 0.4$, $\lambda = 0.8$, and $d = 0.2$. We do not use turbulent resistance term ($\alpha_t = 0$) because this term dissipates wave energy to almost zero after very short distance, i.e., 0.5 wavelength.

We do not have available exact solution for Cnoidal waves propagating inside porous media so we use quasi-exact solution as

$$\eta_q = \eta^I \exp\left(-k_i x\right) \tag{61}$$

Fig. 4 compares numerical and quasi-exact solution. Though numerical solution appears a little bit underestimate, it shows good trend of energy dissipation over computation domain.

Interaction of solitary waves with porous breakwater

Solitary wave can keep its stable form while travelling for a long distance or even when it propagates inside porous media or interact with porous breakwater. In this part we simulate solitary waves interacting with porous breakwater.

Initial and boundary conditions

The solitary wave profile and the corresponding velocity are given by Wang (1993) as

$$\eta = \frac{a}{1+\dfrac{a}{h}}\left[\operatorname{sech}^2 K\left(x - Ct - x_0\right) + \frac{a}{h}\operatorname{sech}^4 K\left(x - Ct - x_0\right)\right] \tag{62}$$

$$u = Kh\sqrt{\frac{4}{3}ga}\,\operatorname{sech}^2 K\left(x - Ct - x_0\right) \tag{63}$$

where x_0 is the initial location of solitary, and

$$K = \frac{1}{h}\sqrt{\frac{3}{4}\frac{\dfrac{a}{h}}{\left(1+\dfrac{a}{h}\right)}} \tag{64}$$

$$C = \sqrt{g(h+a)}$$

(65)

Liu and Wen (1997) and other authors used two types of governing equations to generate waves propagating through a porous breakwater. One is to generate waves outside the porous breakwater and the other for waves inside the porous breakwater. That's why along the interface between the open-water and the porous breakwater they need to apply matching conditions for both free surface displacement and velocity. The free surface and velocity as well as their spatial derivatives are continuous across the interfaces. However, in our study, in order to simulate waves propagating through a permeable breakwater we use only one type of the derived governing equations for waves propagating inside and outside porous media by adjusting the media porosity. That is, outside the breakwater (clean water area) we equate the porosity as unity and inside the breakwater (porous media) we equate the porosity less than unity, as can be seen in Fig. 5. So we do not need any matching conditions at the interface between the open-water and the porous breakwater.
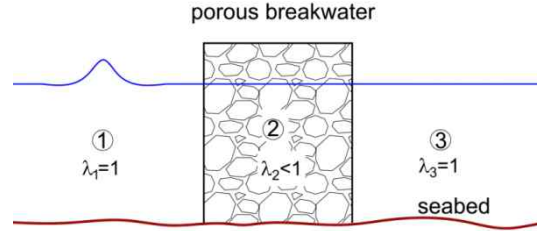

Figure 5. Boundary condition at porous breakwater

Determination of drag coefficient inside porous breakwater

In order to determine the drag resistance term in Eq. (7) we need to specify the velocity inside porous media. Since the horizontal length scale of the solitary wave is much longer than the porous breakwater width, Madsen (1974) assumed the horizontal velocity as constant inside the porous breakwater. For representative velocity they used the averaged discharge velocity ($\bar{u}$) inside the porous breakwater which is given by

$$\bar{u} = \frac{1}{2}(u_0 + u_b)$$

(66)

where u_0 and u_b are the velocities at the up-wave and down-wave ends of the breakwater, respectively.

Based on the assumption of linear variation of the velocities inside the breakwater, Liu and Wen (1997) and Lynett et al. (2000) used the characteristic velocity (U_c) given by

$$U_c = \frac{3}{4}\frac{u_b^4 - u_0^4}{u_b^3 - u_0^3}$$

(67)

This assumption is correct if the width of the breakwater is very thin as shown in Fig. 6(a). However, if the width increases, the velocity distribution inside porous breakwater becomes nonlinear as shown in Fig. 6(b).

By applying one type of the governing equations to the whole domain our present model can determine exactly the velocity at each point inside porous breakwater at each time step as shown in Fig. 7. Applying this advantage, the drag coefficient which is determined in eq. (7) is not constant inside the porous breakwater but depends on varying velocity inside the breakwater.

Interacting of solitary waves to a porous breakwater

Fig. 7 gives us some information for the propagation of solitary waves through a rectangular porous breakwater at several time steps. The incident solitary wave partially passes through and reflects back from the breakwater. The porosity characteristics of the porous breakwater are specified as $\lambda = 0.44$, $\alpha_l = 1092$, $\alpha_t = 0.81$, $d = 2.34\,cm$, the width of the breakwater $b = 20\,cm$. The nonlinearity parameter is $a/h = 0.1$. Our model shows good agreement with Liu and Wen (1997) for the reflected

waves while the transmitted wave amplitude is a little lower than the value of Liu and Wen (1997). The shapes of the transmitted and reflected waves are similar to the solitary wave. The x-coordinate is scaled by $\sqrt{h^3 / a}$, η by a and t by $h / \sqrt{ga}$. Fig. 7(f) shows a small wave tail from the reflected waves because of the frequency dispersion.
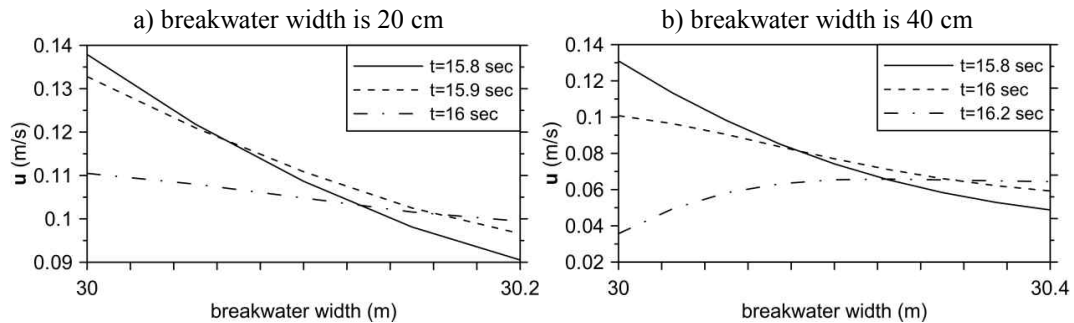

Figure 6. Velocity distribution inside breakwater at different time steps
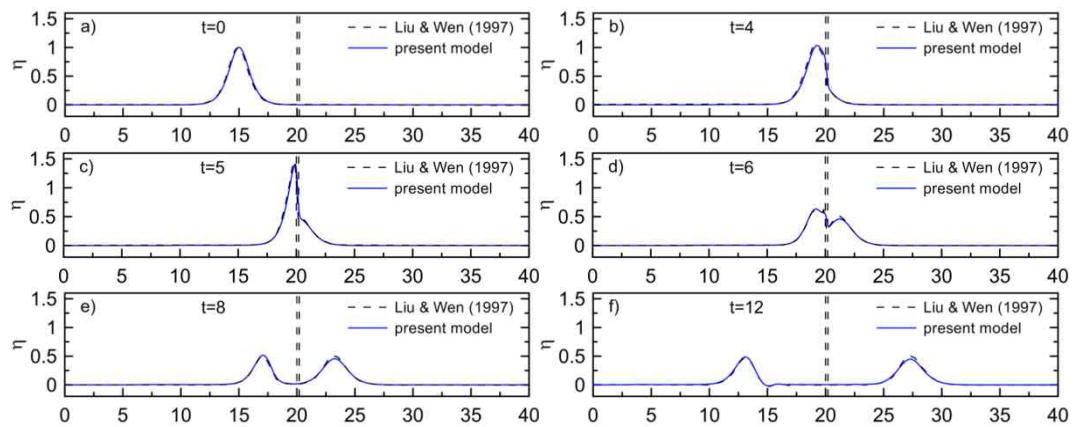

Figure 7. Propagation of solitary wave through a porous breakwater

We verify our numerical transmission and reflection coefficients of solitary waves with the data from Lynett et al. (2000) as shown in Fig. 8. They used the governing equations of Liu and Wen (1997) for waves propagating inside the porous media. They used the solitary initial condition of Wang (1993) and they did their own physical experiment in a wave tank of 30 m length. Solitary waves with amplitude of $1 \sim 3.5$ cm were generated in constant water of 10 cm which results the nonlinearity $a / h = 0.1 \sim 0.35$, and the surface elevations were measured 1 m in front of and 1 m behind the porous breakwater. Breakwater widths are 15 cm and 30 cm. We use their best fit laminar and turbulent drag coefficients as $\alpha = 1100, \beta = 0.81$, respectively for our numerical simulation.

For all 4 cases, the transmission of the present model shows good agreement with Lynett et al. (2000). However, with small nonlinearity (i.e. $\varepsilon < 0.2$) the present model underestimates the reflection coefficient while Lynett et al. (2000) overestimates with high nonlinearity (i.e. $\varepsilon > 0.2$).
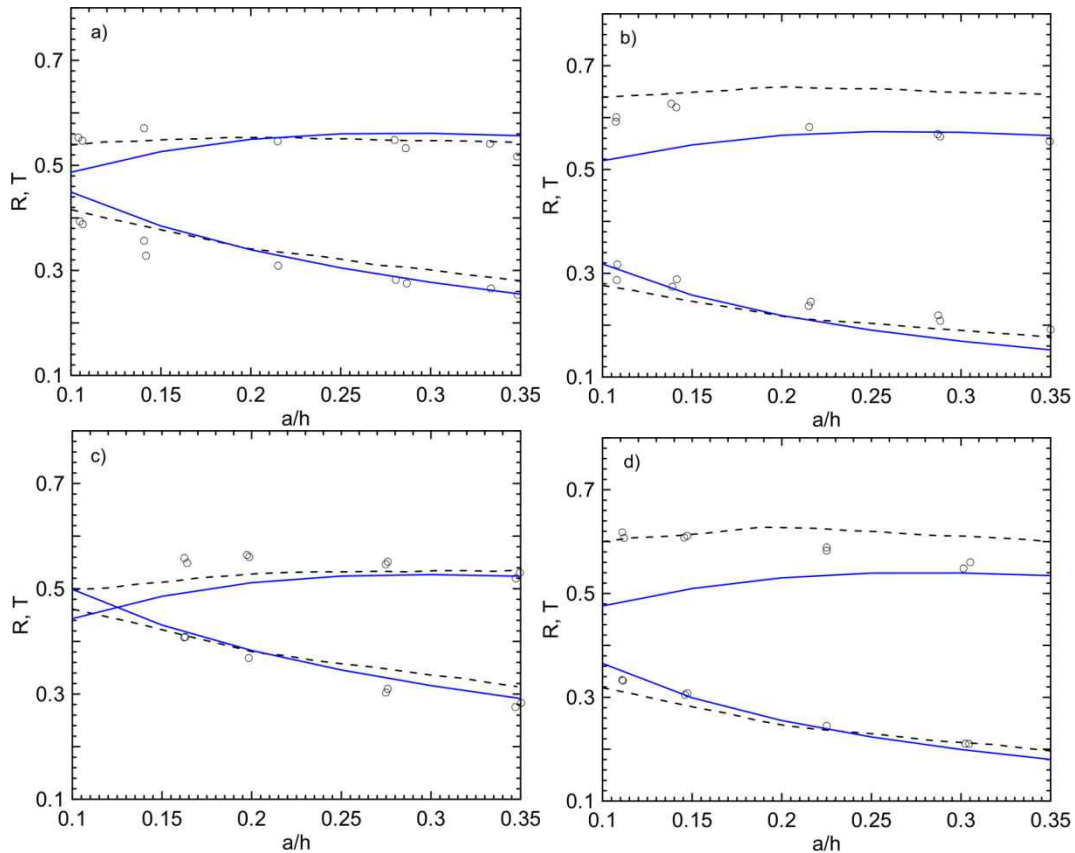
Figure 8. Reflection and transmission of solitary waves by porous breakwater. (a) d=1.6 cm, b=15 cm; (b) d=1.6 cm, b=30 cm; (c) d=2 cm, b=15 cm; (d) d=2 cm, b=30 cm. Line definition: dashed-line = Lynett et al.'s (2000) model; symbols = Lynett et al.'s (2000) experimental data; solid line = present model

CONCLUSIONS

In this research, a new set of the extended Boussinesq equations has been derived to describe wave propagation in porous media. The momentum equation includes drag and inertial resistances. This model can simulate water waves propagating inside and outside porous media simultaneously.

Using internal generation of wave technique, the developed model simulated waves in deep and shallow waters and shown good results when comparing with the analytical solution. Using this model, we generated Cnoidal waves in porous media and compared with the assumed analytical solution and showed good agreement. Further, the model was verified by simulating nonlinear solitary waves. When interacting with permeable breakwater, the solitary waves propagated through permeable breakwater and reflected back from the breakwater. The transmission and reflection coefficients are compared to the available experimental data.

The model is also applied to horizontal two-dimensional domain for linear and nonlinear waves. The numerical results show good agreement with analytical solution and experimental data.

ACKNOWLEDGEMENT

REFERENCES

Cho, Y.-S., 2003. A note on estimation of the Jacobian elliptic parameter in cnoidal wave theory. *Ocean Engineering* 30, 1915-1922.

Cruz, E.C., Isobe, M., Watanabe, A., 1997. Boussinesq equations for wave transformation on porous beds. *Coastal Engineering* 30, 125-156.

del Jesus, M., Lara, J.L., Losada, I.J., 2012. Three-dimensional interaction of waves and porous coastal structures. Part I: Numerical model formulation. *Coastal Engineering* 64, 57-72.

Ergun, S., 1952. Fluid flow through packed columns. *Chemical Engineering Progress* 48, 89-94.

Forchheimer, P., 1901. Wasserbewegung durch boden. Z. Ver. Deutsch. *Ing.* 45, 1782-1788.

Gu, Z., Wang, H., 1991. Gravity waves over porous bottoms. *Coastal Engineering* 15, 497-524.

Hsiao, S.-C., Liu, P.L.-F., Chen, Y., 2002. Nonlinear water waves propagating over a permeable bed. *Proceeding of Royal Society of London A* 458, 1291-1322.

Hsiao, S.-C., Hu, K.-C., Hwung, H.-H., 2010. Extended Boussinesq equations for water-wave propagation in porous media. *J. Engineering Mechanics* 136(5), 625-640.

Kennedy, A.B., Chen, Q., Kirby, J.T., Dalrymple, R.A., 2000. Boussinesq modeling of wave transformation, breaking, and runup. Part 1. *J. Waterway, Port, Coastal and Ocean Engineering* 126(1), 39-47.

Kirby, J.T., Wei, G., Chen, Q., Kennedy, A.B., Dalrymple, R.A., 1998. Fully Nonlinear Boussinesq Wave Model. User's Manual. *CACR Report no. 98-06. Center for Applied Coastal Research, Univ. of Delaware.*

Liu, P.L.-F., Wen, J., 1997. Nonlinear diffusive surface waves in porous media. *J. Fluid Mechanics* 347,119-139.

Liu, P.L.-F., Lin, P., Chang, K.A., Sakakiyama, T., 1999. Numerical modeling of wave interaction with porous structures. *J. Waterway, Port, Coastal, and Ocean Engineering* 125 (6), 322-330.

Liu, Y., Li, H.-J., 2013. Wave reflection and transmission by porous breakwaters: A new analytical solution. *Coastal Engineering* 78, 46-52.

Lynett, P.J., Liu, P.L.-F, Losada, I.J., 2000. Solitary wave interaction with porous breakwaters. *J. Waterway, Port, Coastal, and Ocean Engineering* 126(6), 314-322.

Madsen, O.S., 1974. Wave transmission through porous structures. *J. Waterways, Harbors and Coastal Engineering Division* 100(WW3), 169-188.

Ma, G., Shi, F., Hsiao, S.,-C., Wu, Y.-T., 2014. Non-hydrostatic modeling of wave interactions with porous structures. *Coastal Engineering* 91, 84-98.

Madsen, P.A., Sørensen, O.R., 1992. A new form of the Boussinesq equations with improved linear dispersion characteristics. Part 2. A slowly-varying bathymetry. *Coastal Engineering* 15, 371-388.

Madsen, P.A., Sørensen, O.R., Schäffer, H.A., 1997. Surf zone dynamics simulated by a Boussinesq type model. Part 1. Model description and cross-shore motion of regular waves. *Coastal Engineering* 32, 255-287.

Nwogu, O., 1993. Alternative form of Boussinesq equations for nearshore wave propagation. *J. Waterways, Harbors and Coastal Engineering* 119(6), 618-638.

Peregrine, D.H., 1967. Long waves on beach. *J. Fluid Mechanics* 27, 815-827.

Sollitt, C.K., Cross, R.H., 1972. Wave transmission through permeable breakwater. *Proceeding of 13th International Conference on Coastal Engineering*, ASCE 1827-1846.

Wang, K.-H., 1993. Diffraction of solitary waves by breakwaters. *J. Waterway, Port, Coastal, and Ocean Engineering* 119(1) 49-69.

Wei, G., Kirby, J.T., Grill, S.T., Subramanya, R., 1995. A fully nonlinear Boussinesq model for surface waves. Part 1. Highly nonlinear unsteady waves. *J. Fluid Mechanics* 294, 71-92.

Wei, G., Kirby, J.T., Sinha, A., 1999. Generation of waves in Boussinesq models using a source function method. *Coastal Engineering* 36, 271-299.